

Affected zone generated around the erosion pit on carbon steel surface at the incipient stage of vibration cavitation

CHEN HaoSheng^{1†}, LI Jiang², LIU ShiHan¹, CHEN DaRong¹ & WANG JiaDao¹

¹ State Key Laboratory of Tribology, Tsinghua University, Beijing 100084, China;

² Mechanical Engineering School, University of Science and Technology Beijing, Beijing 100083, China

The characteristics of erosion pits on a carbon steel surface were investigated at the incipient stage of cavitation erosion. After a 5-minute experiment performed in an ultrasonic vibration system, needle-like erosion pits appeared on the polished steel surface, and a specially affected zone was formed around the pit. The shape of the pit and the plastic deformation of the affected zone indicate that the mechanical impact on the surface is the main reason for the cavitation damage. On the other hand, the iridescent color, the decreased surface hardness and the precipitated carbides on the affected zone prove that the affected zone has experienced a tempering process with the temperature higher than 300°C. The lack of oxygen in the affected zone also proves that it is not a chemical oxygen result. A special phenomenon that a carbon ring forms in the affected zone is explained as a result of the toroidal bubbles' heating effect at the final stage of the bubble collapse.

cavitation, cavitation erosion, thermal effect, carbon, ultrasonic vibration

It is commonly agreed that the micro-jet and shock wave caused by a collapsing bubble in water is the main reason for the cavitation erosion on the solid surfaces^[1]. On the other hand, the damage process is often accompanied by the thermal effect. It has been numerically calculated by Plesset^[2] and experimentally validated by Nowotny^[3] and Gavranek et al.^[4] that a high temperature is reached in the cavity at the final stage of collapse. The temperature is so high that the metal strength is reduced and the surface material even melts, which makes the surface easier to be damaged. Numerical results given by Wu et al.^[5] and Ying et al.^[6] recently show that the temperature in the cavity reaches 10000°C at the moment of collapsing. However, the thermal effect is not considered as the main reason for the cavitation erosion. Knapp et al.^[7] have pointed out that the metal surface melts only when the cavity contacts with the solid surface, otherwise the heat is hard to be conducted to the surface effectively. Knapp et al.^[7] also believed that the surface of some materials with good heat conductivity cannot reach a

high temperature, and the colour changed on the metal surface that was once believed to be the result of the thermal effect is now considered as a chemical action under lower temperature.

According to the studies mentioned above, high temperature does exist during the bubble collapse process, but it does not seem to affect the cavitation erosion. In the undergoing study, the characteristics of an erosion pit at the incipient stage of the cavitation erosion are observed to investigate how the erosion pit forms and whether the thermal effect takes part in the formation of the pit. A medium carbon steel sample (0.45% carbon) is installed on a static platform and the bubbles generated by an ultrasonic vibration system rush forward to the sample surface. After a 5-minute experiment, surface

Received June 19, 2007; accepted September 20, 2007

doi: 10.1007/s11434-008-0105-z

†Corresponding author (email: chenhs@mail.tsinghua.edu.cn)

Supported by the National Natural Science Foundation of China (Grant No. 50505020) and the National Basic Research Program of China (Grant No. 2007CB707702)

profile, surface hardness and elemental composition of the polished steel surface are tested, and the damage mechanism of the cavitation erosion is discussed.

Figure 1(a) shows the schematic of an ultrasonic vibration cavitation apparatus used in the experiment. The vibration horn performs an axial vibration with a frequency of 20 kHz and an amplitude of 6 μm . The sample piece is installed on the support arm of a two-dimensional table, and the testing surface faces the tip of the vibration horn. The interval between them is adjusted by the translation stage, while the pitch angle of the sample surface is adjusted by the rotation stage. During this experiment, the distance between the two faces was 15 mm. The experiment is performed in a beaker filled with de-ionized water. Figure 1(b) and (c) show the system before and during the experiment, respectively.

The sample is designed according to the Chinese standard (GB6383-86) on a vibration cavitation erosion system, and its dimension is shown in Figure 2(a). The sample is made of a medium carbon steel (0.45% car-

bon), whose yield point is higher than 680 MPa. The sample surface is polished, and the root mean square (Rms) value of the surface roughness is 12.5 nm, which is tested by an Atomic Force Microscope (AFM) CSPM 4000. It should be noted here that there are three measuring regions on the sample surface marked as 1–3 in Figure 2(b). The size of each region is 5 μm \times 5 μm , and the surface roughness of the sample surface is the mean value of the surface roughness measured in the three regions. Figure 2(c) shows one of the tested regions.

The experiment lasted 5 min. The reason for such a short time was to reduce other damages such as corrosion and abrasion. The cavitation phenomena captured by a digital camera is shown in Figure 1(c). A clear cavitation domain is found near the vibration horn's tip, and some bubbles are seen rushing to the sample surface. Scanning Electron Microscope (SEM, Quanta 200 FEG, FEI Co.) pictures in Figure 3 show the erosion pits on the sample surface with the magnitudes of 300, 2000, and 20000, respectively. It is found in Figure 3(a) that

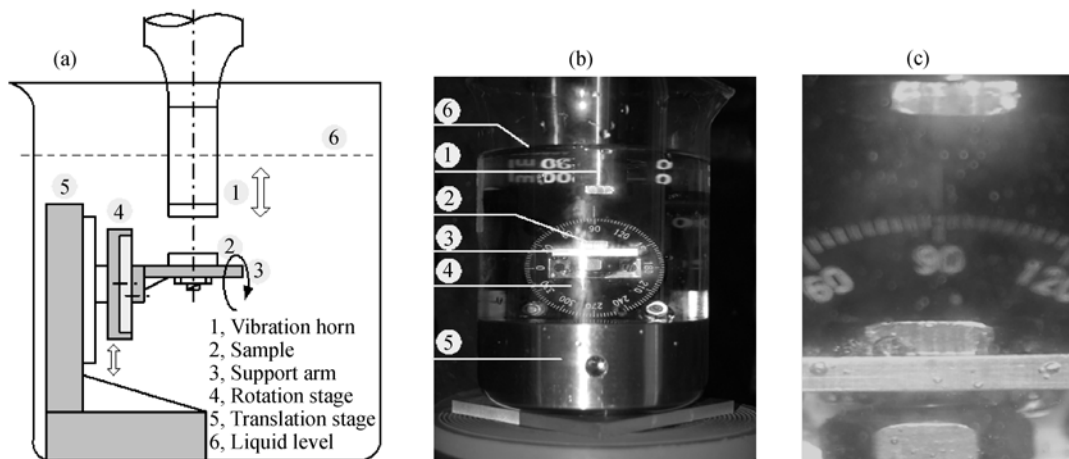


Figure 1 (a) Schematics of the vibration cavitation apparatus; (b) the picture of the apparatus and (c) picture of the system in operation showing cavitation cloud.

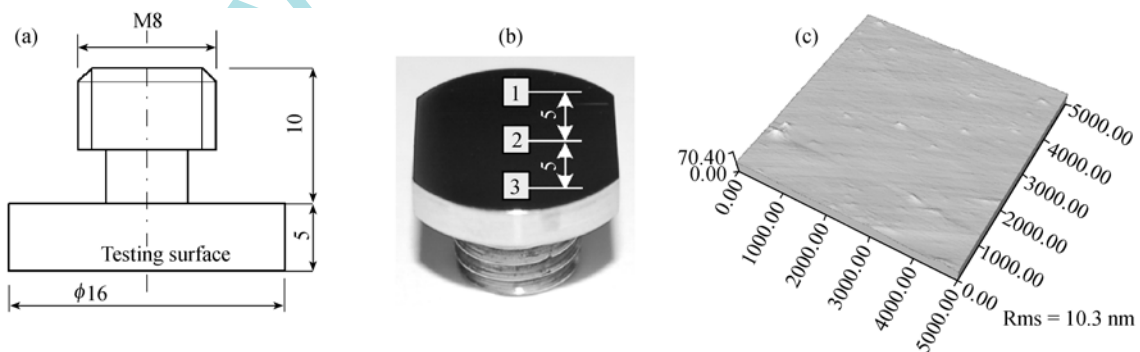


Figure 2 Sample and the tested surface profile. (a) Sample dimension; (b) sample picture; (c) tested sample surface.

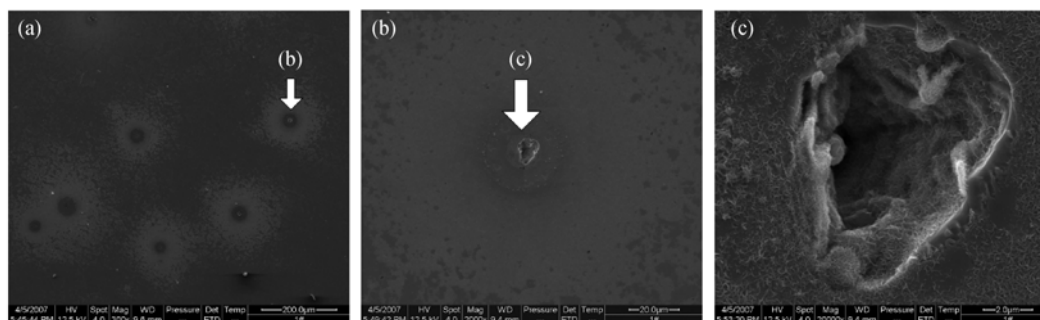


Figure 3 Erosion pits on the sample surface observed by SEM after the experiment with magnitudes of (a) 300, (b) 2000 and (c) 20000.

the erosion pits scatter on the sample surface, and they have two main characteristics:

(i) The pit is deep and small as shown in Figure 3(c), and it is usually called a needle-like pit. It is a characteristic phenomenon appearing at the incipient stage of the cavitation erosion as described by Hammit^[1], and it is considered as the result of a micro-jet impacting on the surface at the moment of the bubble collapse.

(ii) As shown in Figure 3 (a) and (b), an obvious affected zone in deep color can be seen around each erosion pit. An erosion pit with an obvious affected zone was chosen and observed by an Olympus LEXT OLS3100 confocal laser scanning microscope. In Figure 4, the affected zone surrounded the erosion pit has a distinguished round shape. The continuous line represents the surface profile of the surface at the cross-section marked by the dashed line. The line is across the center of the erosion pit, and the surface profile shows both the shapes of the pit and of the affected zone. The erosion pit is narrow and deep, while the affected zone is obviously raised from the base, whose shape looks like the rise ring on the aluminum surface in the erosion experiment done by Knapp^[8]. The affected zone is believed to

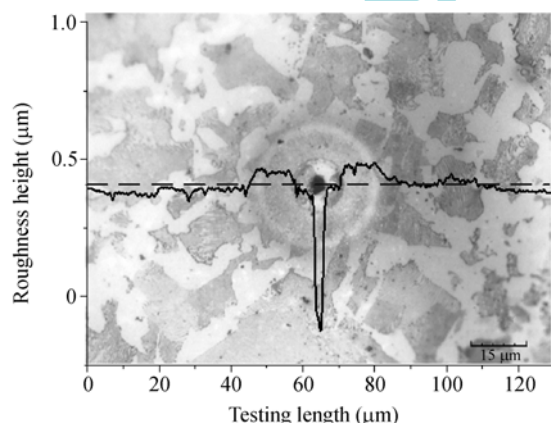


Figure 4 Surface profile of the erosion pit with the affected zone tested by the confocal laser scanning microscope.

be the plastic deformation of the material following the impaction happening in the pit's center at the moment of the bubble collapse. So both the formation of the erosion pit and the deformation of the affected zone indicate that a mechanical action with high pressures is the main damage mechanism for the cavitation erosion, which also agrees with Plesset's viewpoint^[9].

The hardness of the affected zone was tested by a Nano Tester (MML Co.). 25 indents were made on the sample surface outside the pit along the radius direction, which are shown in Figure 5(a). The interval between the two indents is 1 μm. The maximum indent depth is 800 nm, and the maximum load is 20 mN. The hardness of the surface within and outside the affected zone is shown in Figure 5(b). It is found that the average value of the hardness in the affected zone is approximate half of that outside the affected zone.

Another important phenomenon is that the affected zone appearing in the optical microscope is colorful. Moreover, as shown in Figure 4 and Figure 5(a), the color of the surface at the edge of the zone changes from red to blue gradually. The appearance of the iridescent color indicates that the temperature on the steel surface may reach 300°C according to the experiment of Wang et al.^[10]. In addition, it is known that the hardness of the medium carbon steel decreases when the steel is tempered at the temperature higher than 300°C. So, the iridescent color and the decreased surface hardness both indicate that the affected zone has experienced a high temperature tempering process.

Based on the heat treatment theory^[11], the surface hardness reduction during the tempering process is caused by the precipitation of the carbides on the surface. Therefore, the elemental composition of surface materials on the damaged surface was tested by an EPMA-1600 electronic probe with a wavelength dispersive spectrometry (WDS). The elements of Ferro, carbon and

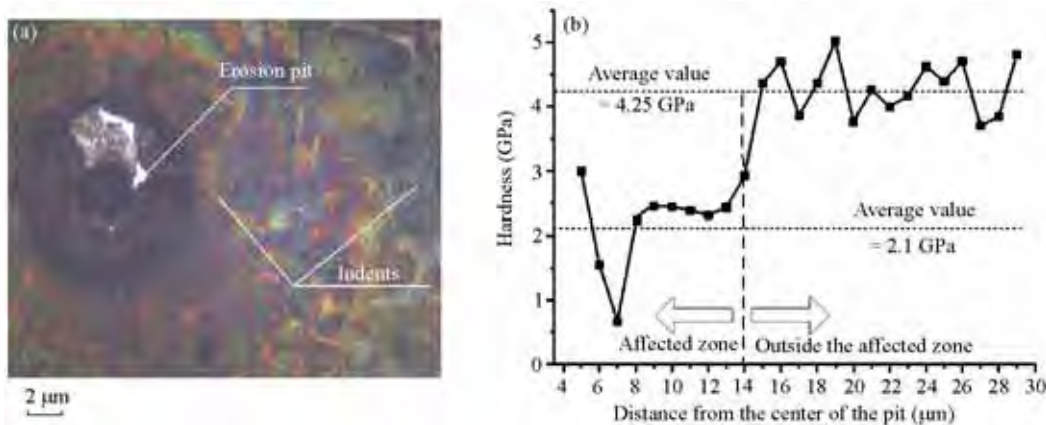


Figure 5 Surface hardness testing. (a) is the pit with indents; (b) is the hardness in and outside the affected zone.

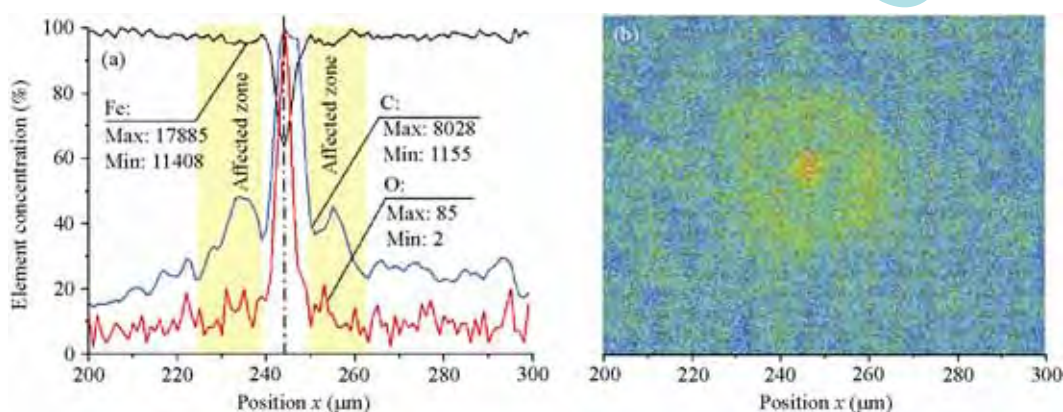


Figure 6 The elemental composition of surface materials tested by an EPMA-1600 electronic probe. (a) The line scan results of Fe, C and O; (b) the area scan result of carbon.

oxygen within the affected zone were detected. The concentrations of the three different elements are shown in Figure 6(a) using line scan along the horizontal diametric line. The Y axis represents the percentage of each element compared with its maximum atom counts, while the numbers marked in the figure are the true maximum and minimum atom counts for each element.

Two main phenomena are found from the detected results. First, in the erosion pit, the Ferro concentrations decrease while the concentrations of carbon and oxygen increase. Second, the carbon concentration in the affected zone obviously increases although such a concentration is much lower than that in the erosion pit. This phenomenon can be seen more clearly in Figure 6(b). In Figure 6(b), the distribution of the carbon on the damaged surface is tested using the area scan method, where the concentration is represented by the color. Besides the carbon aggregation in the erosion pit, the carbon also forms a ring in the affected zone, which is called the 'carbon ring' here. It is proved now that the carbon and

carbides precipitate on the surface, and the affected zone has experienced a tempering process. Moreover, the temperature distribution in the affected zone can be qualitatively described because the precipitated carbides grow on the steel surface as the temperature increases. As a result, the sequenced regions according to the temperature from high to low are the pit, the carbon ring, and the affected zone between them. It is easy to understand why the temperature in the pit is the highest, because energy released at the moment of the bubble collapse acts on the surface and forms the erosion pit through the micro-jet with high temperature and high speed. The temperature is so high that the surface material may be burned, and that is why the oxygen concentration increases only within the pit. The lack of oxygen outside the pit also indicates that the affected zone is not a chemical oxygenized result under lower temperature. The formation of the carbon ring is considered here to be related to the bubble profile at the final stage of the collapse near the surface. The numerical results acquired

by Best^[12] and Zhang et al.^[13] show that a bubble will change its shape from spherical to toroidal after the first collapse, and the temperature in the toroidal bubble is still high. Because the affected zone is raised after the first impactation caused by the micro-jet, its surface is closer to the toroidal bubble or even contacts it, then the surface is tempered with higher temperature at the place where the ring forms than in other regions between the ring and the pit.

Ultrasonic vibration cavitation erosion experiment was performed on a polished 45# carbon steel surface for 5 min. The characteristics of the pits at the incipient stage of the cavitation erosion were investigated. And some of the conclusions are drawn as follows:

(i) The surface profile of the damaged surface shows that a raised affected zone is formed around each characteristic needle-like pit. The narrow and deep profile of

the pit and the plastic deformation of the affected zone indicate that the mechanical impactation is the main reason for the cavitation erosion at the incipient stage.

(ii) The iridescent color, the surface hardness reduction and the precipitated carbides on the surface all indicate that the affected zone has experienced a tempering process with a temperature higher than 300°C. The lack of oxygen in the affected zone also proves that it is not a chemical action under lower temperature. The aggregation of the carbon at the pit is thought to be caused by the high temperature generated at the moment of the bubble collapse, while the carbon ring is considered to be caused by the heating effect of the toroidal bubble on the affected zone at the final stage of the bubble collapse.

The authors would like to thank Yang Wenyan (Tsinghua University) for her contributions toward this work.

- 1 Hammit F G. Cavitation and Multiphase Flow Phenomena. New York: McGraw-Hill, 1980. 241
- 2 Plesset M S, Bubble D. Cavitation in Real Fluids. New York: Elsevier Publishing Co., 1964
- 3 Nowotny H. Destruction of Materials by Cavitation. Berlin: VDI-Verlag, 1942
- 4 Gavranek V V, Bol'shutkin D N, Zel'dovich V I. Thermal and mechanical action of a cavitation zone on the surface of a metal. Fiz Metal I Metalloved, 1960, 10: 262—268
- 5 Wu C C, Robert P H. Shock-wave propagation in a sonoluminescence gas bubble. Phys Rev Lett, 1993, 70(22): 3424—3427
- 6 Ying C F, An Y. High temperature and high pressure distribution in gas bubbles generated by sound cavitation. Sci China Ser A-Math, 2002, 45(7): 926—936
- 7 Knapp R T, Daily J W, Hammit F G. Cavitation. New York: McGraw – Hill, 1970
- 8 Knapp R T. Recent investigations of cavitation and cavitation damage. Trans ASME, 1955, 77: 1045—1054
- 9 Plesset M S, Ellis A T. On mechanism of cavitation damage. Trans ASME, 1955, 77: 1055—1064
- 10 Wang Z C, Zhang Y, Zhang X Q. Thermal effect of cavitation erosion. Chin J Mater Res, 2001, 15(3): 287—290
- 11 Gregory E, Simons N. The Heat-Treatment of Steel. London: Pitman & Sons, Ltd., 1958
- 12 Best J P. The formation of toroidal bubbles upon the collapse of transient cavities. J Fluid Mech, 1993, 251: 79—107
- 13 Zhang S, Duncan J H, Chahine G L. The final stage of the collapse of a cavitation bubble near a rigid wall. J Fluid Mech, 1993, 257: 147—181